Hybrid Aerogel SiNP Membranes for Photocatalytic Remediation of Oil Sands Process Water

Muhammad Iqbal, Tapas K. Purkait, Maryam Aghajamali, Lida Hadidi and Jonathan G.C. Veinot

Department of Chemistry, University of Alberta

Greg G. Goss

Department of Biological Sciences, University of Alberta

Mohamed Gamal-El-Din and James R. Bolton

Department of Civil and Environmental Engineering, University of Alberta

November 2014

Oil Sands Research and Information Network

The Oil Sands Research and Information Network (OSRIN) is a university-based, independent organization that compiles, interprets and analyses available knowledge about managing the environmental impacts to landscapes and water impacted by oil sands mining and gets that knowledge into the hands of those who can use it to drive breakthrough improvements in regulations and practices. OSRIN is a project of the University of Alberta's School of Energy and the Environment (SEE). OSRIN was launched with a start-up grant of $4.5 million from Alberta Environment and a $250,000 grant from the Canada School of Energy and Environment Ltd.

OSRIN provides:

- **Governments** with the independent, objective, and credible information and analysis required to put appropriate regulatory and policy frameworks in place
- **Media, opinion leaders and the general public** with the facts about oil sands development, its environmental and social impacts, and landscape/water reclamation activities – so that public dialogue and policy is informed by solid evidence
- **Industry** with ready access to an integrated view of research that will help them make and execute environmental management plans – a view that crosses disciplines and organizational boundaries

OSRIN recognizes that much research has been done in these areas by a variety of players over 40 years of oil sands development. OSRIN synthesizes this collective knowledge and presents it in a form that allows others to use it to solve pressing problems.

Citation

This report may be cited as:

Iqbal, M., T.K. Purkait, M. Aghajamali, L. Hadidi, J.G.C. Veinot, G.G. Goss and M. Gamal El-Din, 2014. Hybrid Aerogel SiNP Membranes for Photocatalytic Remediation of Oil Sands Process Water. Oil Sands Research and Information Network, University of Alberta, School of Energy and the Environment, Edmonton, Alberta. OSRIN Report No. TR-54. 29 pp.

Copies of this report may be obtained from OSRIN at osrin@ualberta.ca or through the OSRIN website at http://www.osrin.ualberta.ca/en/OSRINPublications.aspx or directly from the University of Alberta's Education & Research Archive at http://hdl.handle.net/10402/era.17507.

Table of Contents

LIST OF TABLES

LIST OF FIGURES

REPORT SUMMARY

There are many candidate technologies that could be applied to the treatment of oil sands process-affected water (OSPW). Advanced oxidation processes (AOPs) are particularly useful for degrading biologically toxic or non-degradable materials such as aromatics, pesticides, petroleum constituents, and volatile organic compounds in wastewater.

AOPs based on photocatalysis using nanomaterials are promising due to the high surface area, and exquisite tunability of surface chemistry afforded by the nanoparticles as well as the potential for harnessing sunlight as a passive, cost-effective energy source to initiate the reactions. However, application of these attractive materials in large-scale operations remains a challenge. To address these challenges, photocatalytic reactors have been proposed that utilize nanoparticle slurries or nanoparticles immobilized on various membrane supports. Ceramic membranes are often preferred because of their thermal and chemical stability. Recently, another class of support known as aerogels has attracted attention in absorption-based remediation. To date, there is a lack of reports in which these materials or nanomaterial hybrids have been applied as photocatalytic membranes.

In this report, we present new hybrid silica aerogels that contain Si nanoparticles (SiNPs). The aerogels are produced using versatile and straightforward sol-gel reactions in the presence of SiNPs. Monoliths of the final SiNP-containing aerogel are obtained after drying in supercritical CO_2 and have extremely high surface areas (>1,000 m^2/g) as well as uniform and narrow pore structures. These hybrid aerogels offer distinct advantages of low density, high surface while maintaining the characteristics of immobilized SiNPs.

ACKNOWLEDGEMENTS

The Oil Sands Research and Information Network (OSRIN), School of Energy and the Environment (SEE), University of Alberta provided funding for this project.

The authors would like to thank Wayne Moffat and Jennifer Jones at the Department of Chemistry, University of Alberta for assistance with the FTIR analysis. Kai Cui at National Institute of Nanotechnology (NINT) is gratefully acknowledged for assistance with the HR-TEM measurements.

1 INTRODUCTION

Nanomaterial-based heterogeneous photocatalysts hold great promise as a cost effective, environmentally-friendly and sustainable water treatment technology. However, technical challenges remain that must be addressed if large-scale implementation of these materials is to be realized, including:

1. catalyst optimization to improve quantum yield;
2. nanomaterial design to allow for utilization of visible light (Zhang et al. 2012);
3. reactor design and optimization;
4. catalyst recovery/immobilization techniques; and
5. introduction of reaction selectivity (Qu et al. 2013, Qu and Duan 2013).

Ideally, photocatalytic reactors should provide uniform irradiation to the catalyst material and maximum interaction with the water being treated. Reactors used for these purposes are commonly classified into two main groups: (1) reactors with nanomaterials (NMs) suspended within the reaction mixture, and (2) reactors with NMs fixed onto (i.e., physiosorbed, chemically bonded, etc.) a support material (e.g., glass, quartz, stainless steel, pumice stone, titanium metal, zeolites, etc.) (Mozia 2010).

When photocatalyst slurries are employed, high volumetric generation rates of reactive oxygen species (ROS) proportional to the number of active surface sites are typically reported (Gogate and Pandit 2004, Pozzo et al. 1997). Given catalytic NMs are often costly, and they themselves may pose the risk of being pollutants, additional post-treatment separation is required. Catalyst recovery can be achieved *via* a variety of processes such as hybridization with conventional sedimentation, cross-flow filtration, or even various membrane filtration methodologies (Chong et al. 2010, Yang and Li 2007, Zhang et al. 2008). However, these procedures often significantly increase operational and maintenance costs.

An attractive alternative to slurry-based systems involves NMs being immobilized in/on inert high surface area substrates; however this too comes with challenges. Generally, reactors of this type are characterized by low surface area-to-volume ratios which limit catalyst accessibility and mass transport, as well as inefficiencies related to the absorption and scattering of light by the reaction medium (Chong et al. 2010, Mozia 2010). There has been a concerted effort to address these challenges by applying new support materials and reactor designs.

1.1 Supports for Photocatalytic Nanomaterials in Water Treatment

Photocatalytic membranes (PMs) bearing immobilized photocatalytic reaction sites are particularly attractive for water treatment because the photocatalytic reaction readily proceeds at the membrane surface while treated water is continuously discharged with negligible loss of photocatalyst (Wang et al. 2013). PMs typically consist of ceramics or polymers however, ceramic membranes are preferred because of their superior thermal properties, and are more

chemically resistant (For example see: Chin et al. 2006, Kwak et al. 2001). There are numerous reports of micron-sized immobilizers (e.g., activated carbon (Lee et al. 2004), mesoporous clays (Chong et al. 2009), nanofibres, nanowires, nanorods (Li et al. 2013, Zhu et al. 2004), or membranes (Kwak et al. 2001, Zaky and Chaplin 2013)) being used to facilitate catalyst fixation. In some cases, enhancement of surface contact with contaminants has been demonstrated (Xi and Geissen 2001, Zhang et al. 2009).

Photocatalytic reactors employing PMs are commonly termed photocatalytic membrane reactors (PMR) (Figure 1) (Mozia 2010). In the PMRs using immobilized NPs, the membrane acts as a support for the photocatalyst and might act as a barrier for the molecules present in the solution (initial compounds and products or by-products of their decomposition). When a photocatalytic membrane is employed, the photodecomposition of the pollutants takes place at the membrane surface or within its pore structure. In this context, it is only necessary to irradiate the membrane (Mozia 2010, Qu et al. 2012).

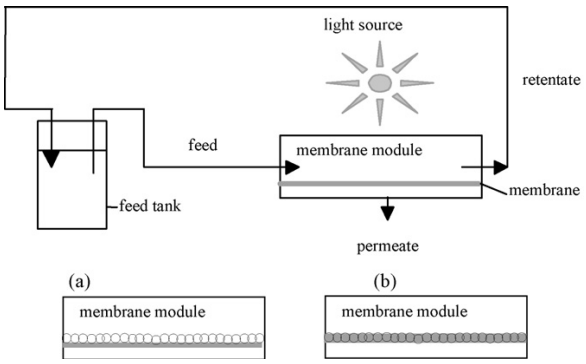

Figure 1. Schematic of a PMR utilizing photocatalyst immobilized (a) on a membrane and (b) within a membrane structure.

As part of our previous work with OSRIN (Iqbal et al. 2013), we established surface modified silicon nanoparticles (SiNPs) as excellent photocatalysts with unprecedented quantum yields (QYs) and yield factors when compared to traditional TiO_2-based systems. We demonstrated that SiNPs can rapidly degrade model contaminants (e.g., methanol) with high efficiency upon exposure to standard UV sources. This project aimed to expand the scope of application of SiNPs by immobilizing them within highly porous substrates and applying these substrates for wastewater treatment. The membranes of choice were silica aerogels because of their chemical compatibility with SiNPs, high surface area, and optical transparency. Water-soluble SiNPs of different sizes were incorporated into the aerogels during sol-gel processing. The aerogels were irradiated with UV light for the degradation of model contaminants.

2 AEROGELS

Aerogels are coherent, porous solids made by the formation of a colloidal gel followed by removal of the solvent trapped within the pores of the gel. Among their attractive properties, aerogels are generally characterized by ultra-low densities (0.004 to 0.5 g/cm^3), high surface areas (1,000 m^2/g), high porosity (75% to 95%), and low thermal conductivities. They can be prepared as monoliths and can also be optically transparent (Gesser and Goswami 1989).

Given their high porosity, surface area and thermal stability, aerogels are ideal materials for applications in environmental remediation. They can be used as adsorbents of organic and inorganic pollutants, and they can be loaded with catalytic nanoparticles capable of pollutant degradation. *Passive* (i.e., non-reactive) carbon-based aerogels have been successfully implemented for the removal of metal ions (e.g., Cd(II), Pb(II), Hg(II), Cu(II), Ni(II), Mn(II) and Zn(II)) (Meena et al. 2005) as well as the adsorption and removal of organic contaminants (phenols, polycyclic aromatic hydrocarbons (PAHs)) (Celzard et al. 2012). *Reactive* aerogels containing silver have been used for removal of halide ions (i.e., Br^-, I^-) which are often difficult to remove using standard procedures (Sánchez-Polo et al. 2006). Hydrophobic silica-based aerogels and xerogels have been used for the removal of model organic pollutants (e.g., phenol, benzene, and toluene) from aqueous solutions (Perdigoto et al. 2012). Aerogels have also been loaded with photocatalytic TiO_2 nanoparticles and applied in the degradation of model contaminants (Jin et al. 2011). Clearly these materials hold promise for remediation of oil sands process-affected water (OSPW).

Unfortunately, the quantum yields reported for the generation of hydroxyl radicals by TiO_2 are comparatively relatively low (i.e., 0.04 to 0.05) (Sun and Bolton 1996). In this context, it is important to explore other semiconductor NP platforms for efficient OSPW remediation. SiNPs offer an excellent TiO_2 alternate; they are environmentally and biologically benign and can exhibit a band gap as high as ca. 2.5 eV. Fortunately, SiNP chemistry is also fully compatible with standard SiO_2-based sol-gel chemistry.

In this report, we present our initial findings of using silica aerogel impregnated with SiNPs for the degradation of model contaminants.

3 SYNTHESIS AND CHARACTERIZATION OF SILICON (Si) NANOPARTICLES

3.1 Synthesis and Characterization of Polymer Intercalated SiNPs

Candidate SiNPs were identified as part of our previous OSRIN-sponsored studies (Iqbal et al. 2013). General procedures for preparing SiNPs are summarized in Figure 2. Briefly, three sizes of SiNPs (i.e., 3NM, 9NM and 75NM[1]) were obtained from thermal processing of hydrogen silsesquioxane (HSQ) (Hessel et al. 2006, Veinot 2006). The largest nanocrystals (i.e., 100NM) were obtained by annealing commercially available d = 100 nm silicon nanopowder (Strem Chemicals, Inc.) in an Argon atmosphere at 1,100 °C.

[1] NM is used in this report as a *name* for the SiNP whereas nm is used as the *unit of measurement*.

Oxide was removed from all SiNPs upon exposure to aqueous hydrofluoric acid (HF). This procedure also provided hydride surface termination that facilitated further modification upon thermally induced hydrosilylation with dodecene (Hessel et al. 2006, 2007). The resulting dodecyl-modified SiNPs were purified using standard procedures and are soluble in common non-polar solvents (Figure 2(b)). Dodecyl-terminated SiNPs were rendered water soluble upon coating/intercalating with a known amphiphilic polymer (Figure 2(c)) (Lin et al. 2008).

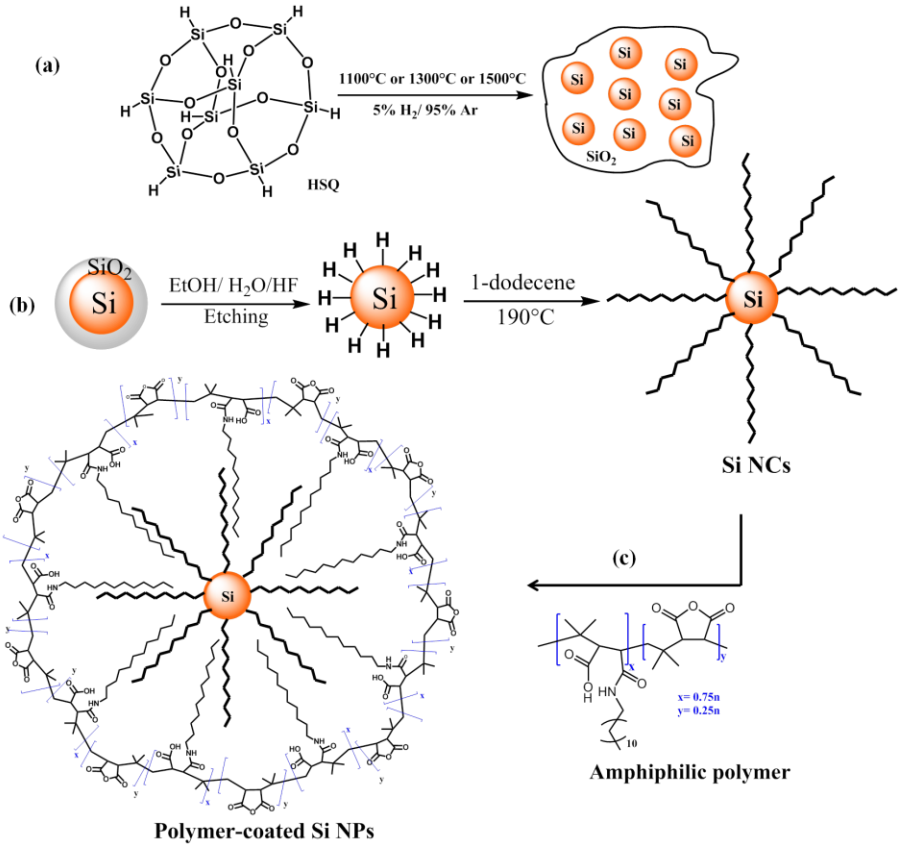

Figure 2. A general scheme for the preparation of water soluble SiNPs.
(a) Synthesis of 3NM and 9NM and 75NM.
(b) Thermal hydrosilylation, and
(c) intercalation with amphiphilic polymer.

3.2 Synthesis and Characterization of Carboxylic Acid (4-Pentenoic Acid)-Terminated SiNPs

Hydride surface-terminated SiNPs obtained from the HF etching procedure as noted in section 3.1 were modified using radical induced hydrosilylation with 4-pentanoic acid (Zhai et al. 2014) as shown in Figure 3. The resulting carboxylic acid-terminated (-COOH) SiNPs were purified using standard procedures and are soluble in polar solvents (i.e., water and low boiling alcohols).

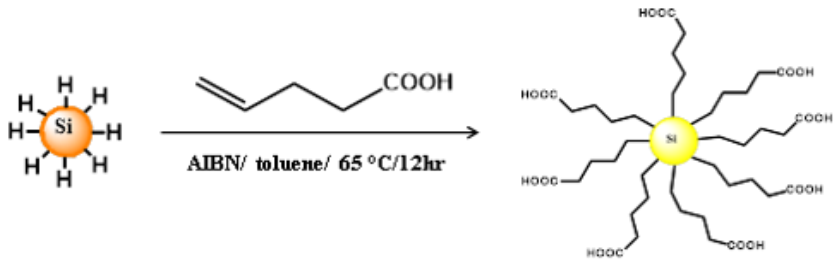

Figure 3. Schematic for the functionalization of SiNPs with 4-pentenoic acid.

3.3 SiNP Characterization

Table 1 lists the SiNP types and sizes used in this study. All SiNPs were comprehensively characterized using photoluminescence (PL), Fourier-Transform Infrared Spectroscopy (FTIR) and Transmission Electron Microscopy (TEM) and High Resolution Transmission Electron Microscopy (HR-TEM).

Table 1. List of SiNPs used in this study.

	3NM	6NM	9NM	75NM	100NM
Dodecyl-modified SiNPs	3NM		9NM	75NM	100NM
Polymer intercalated SiNP	3NM-P		9NM-P	75NM-P	100NM-P
Acid-terminated SiNPs	3NM-Acid	6NM-Acid	9NM-Acid		

4 RESULTS AND DISCUSSION

4.1 Polymer Intercalated SiNPs

FTIR analyses of all dodecyl-modified SiNPs show C–H_x stretching absorptions at 2,957 cm^{-1}, 2,925 cm^{-1}, and 2,853 cm^{-1}, as well as C–CH_3 deformations at 1,464 cm^{-1} and 1,378 cm^{-1}; little evidence of residual Si-H moieties (ca. 2,100 cm^{-1}), and Si-O-Si stretching indicative of surface oxidation (ca. 1,100 cm^{-1}) are observed (Figure 4(a)) (Henderson et al. 2009). The FTIR spectrum of the amphiphilic maleic anhydride polymer shows features readily assigned to ν(C-H) at 2,850 to 2,950 cm^{-1}, as well as a broad absorption centered at 3,300 cm^{-1} arising from ν(N-H) and/or ν(O-H) moieties (Figure 4(b)). Residual anhydride ν(C=O) of the polymer appeared at 1,780 cm^{-1}. Broad absorptions at 1,705 and 1,575 cm^{-1} arise from acid and amide ν(C=O) stretching and δ(N-H) bending, respectively[2].

[2] Absorption of energy in the infrared region (4,000 to 200 cm-1) arises from the changes in the vibrational energy of the molecules. There are two types of vibrations that cause absorptions in an IR spectrum – stretching (ν) and bending (δ) of the chemical bonds.

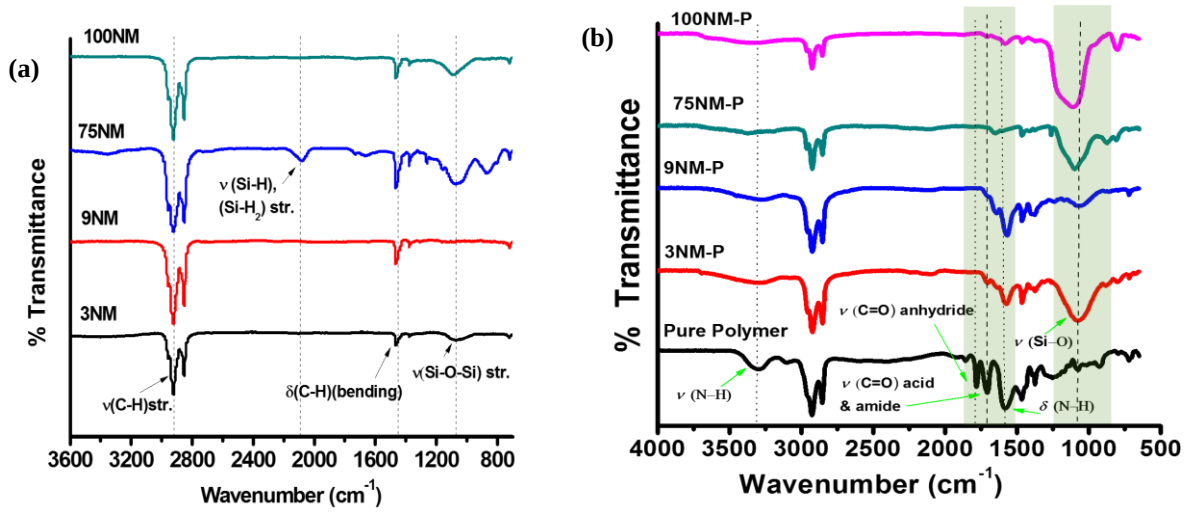

Figure 4. FTIR spectrum of SiNPs.
(a) alkyl-functionalized 3NM, 9NM, 75NM and 100NM SiNPs.
(b) of polymer intercalated 3NM-P, 9NM-P, 75NM-P and 100NM-P SiNPs**.**

The FTIR spectra of polymer coated SiNPs (i.e., 3NM-P, 9NM-P, 75NM-P and 100NM-P, Figure 1) show spectral features corresponding to ν(N-H) (ca. 3,300 cm^{-1}), δ(N-H) (ca. 1,575 cm^{-1}), and amide ν(C=O) (ca. 1705 cm^{-1}). The absorption arising from the anhydride ν(C=O) at 1,780 cm^{-1} was not observed for coated SiNPs.

This observation is consistent with complete hydrolysis of the anhydride groups and supported by a shoulder at 1,645 cm^{-1} that may be confidently assigned to carboxylate ν(C=O) stretching. The 3NM-P and 100NM-P spectra exhibit more intense features arising from ν(Si-O-) stretching at ~1,100 cm^{-1} compared to those observed for 9NM-P and 75NM-P.

The photoluminescence (PL) spectra of aqueous solutions of 3NM-P, 9NM-P, 75NM-P, and 100NM-P were collected upon excitation at 350 nm (Figure 5). 3NM-P exhibited a PL maximum at 692 nm and 9NM-P showed near-IR emission (i.e., 955 nm) while 75NM-P and 100NM-P did not show any detectable PL response.

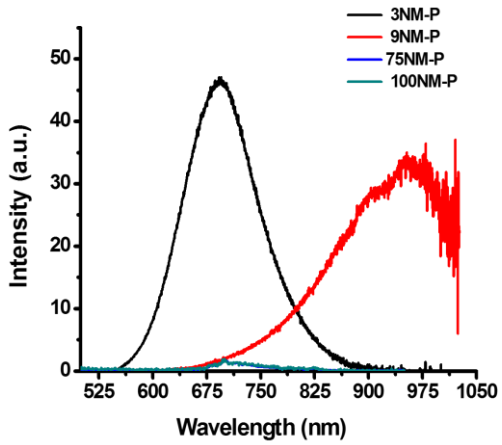

Figure 5. PL-emission spectra of water-soluble SiNPs upon excitation at 350 nm.

TEM provided direct evaluation of SiNP morphology (Figure 6). The dimensions obtained from TEM analysis (d_{3NM} = 2.8 ± 0.4 nm, d_{9NM} = 8.5 ± 1.7 nm and d_{75NM} = 72.6 ± 12 nm) of pseudospherical SiNPs obtained from HSQ-processing depend upon peak thermal processing temperature (Hessel et al. 2007). Evaluation of 3NM and 9NM using HR-TEM (insets Figure 6(a) and (b)) showed lattice fringes spaced by 0.33 nm, which is in close agreement with the bulk atomic plane spacing (i.e., 0.32 nm) for diamond-structured Si and is consistent with other reported Si nanostructures (Kang et al. 2007). SiNPs obtained from HF etching and functionalization of annealed commercial Si nanopowder (i.e., 100NM) showed pseudospherical morphology with average diameters of ca. 103 ± 9 nm (Figure 6d).

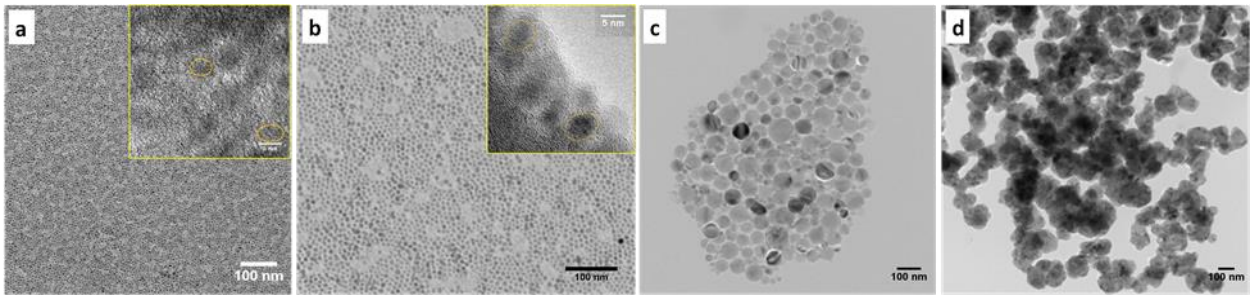

Figure 6. Representative TEM images of SiNPs.
(a) 3NM (b) 9NM (c) 75NM and (d) 100NM. Scale bar = 100 nm.
Insets show appropriate HR-TEM images. Scale bar = 5 nm.

4.2 Carboxylic Acid Terminated SiNPs

FTIR analysis confirmed the SiNPs are functionalized with 4-pentanoic acid after hydrosilylation (Figure 7). The FTIR spectrum shows broad absorptions for ν(O-H) at ~3,400 cm^{-1} and a strong peak at ~1,750 cm^{-1} for υ(C=O) absorptions. The functionalization was further confirmed by the appearance of υ(C-CO-O) absorption at 1,210 cm^{-1} and υ(C-O) at ~1,100 cm^{-1}. It is noteworthy that oxide absorptions υ(Si-O) also appear at 1,100 cm^{-1} so there may be some residual oxide species (Si-O) present. There is negligible residual Si-H_x as evident from the υ(Si-H_x) absorptions which appears at 2,100 cm^{-1}.

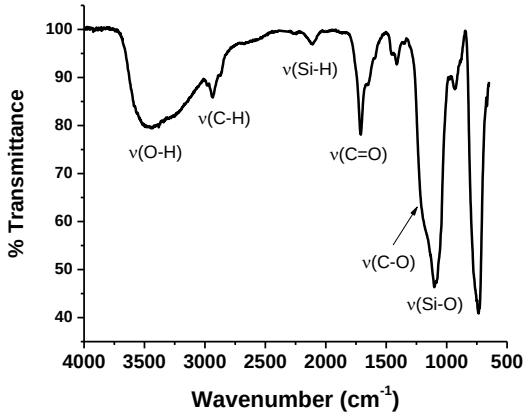

Figure 7. Representative FTIR spectrum of 4-Pentanoic acid functionalized SiNPs.

3NM-Acid SiNPs absorb in the UV and visible range (Figure 8(a)) while 6NM-Acid (red shifted) and 9NM-Acid are expected to absorb in the UV/visible and near-IR spectral range respectively. TEM was employed to evaluate the morphology of the d = 3nm acid functionalized SiNPs. The NPs appear highly aggregated on the TEM grids consistent with the significant H-bonding and possible dimer formation arising from the carboxylic acid surface groups (Figure 8(b)). Limited solubility of larger SiNPs precluded effective TEM analysis.

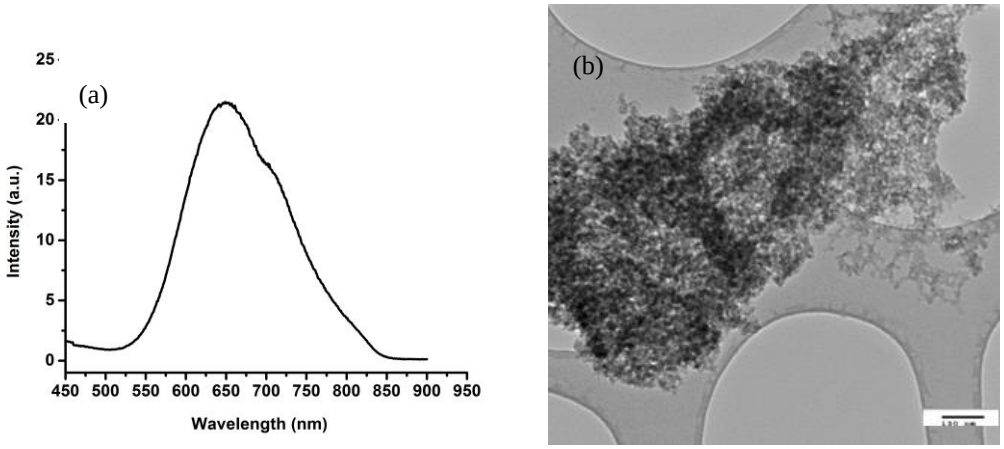

Figure 8. PL and TEM images of 3NM-Acid SiNPs.
(a) PL emission spectra of 3NM-Acid SiNPs upon excitation at 350 nm
(b) representative TEM image of 3NM-Acid SiNPs.
Scale bar =100 nm.

5 SYNTHESIS AND CHARACTERIZATION OF SILICA-BASED AEROGELS

Base-catalyzed silica aerogels were synthesized using a modified literature procedure that required fabrication of a "supercritical dryer" (Anderson et al. 1999, García-González et al. 2012). Briefly, a solution containing 1.97 mL of tetramethoxysilane (TMOS, Aldrich) and 2.26 mL of methanol (MeOH), and catalyst solution containing 2.26 mL of MeOH, 0.76 mL of water, and 2.6 µL of ammonium hydroxide (30%, EMD Chemicals) were mixed and sonicated for 1 min. The mixture was subsequently poured into cylindrical molds, covered, and aged for 1 day. Base-catalyzed silica gels were transferred to glass vials and the solvent was exchanged with anhydrous ethanol (replenishing the solvent every 2 hours for 1 day). The procedure was repeated using acetone at least 8 times over the course of 2 days. The resulting gel was loaded into a home-made supercritical dryer and the acetone was displaced with liquid CO_2. The gel was maintained in liquid CO_2 for ca. 12 hours to ensure maximum displacement of acetone. Finally, the temperature of the dryer was raised to above the critical point of liquid CO_2 (T_c = 31 °C; P_c = 1,071.4 MPa), and the gel was dried under supercritical conditions. For comparison, silica xerogels were also prepared by straightforward solvent evaporation of acetone-exchanged gels over the course of 3 days under ambient conditions.

To investigate the impact of SiNP dimensions on aerogel formation and subsequent reactivity, silica aerogels and xerogels containing pentanoic acid-functionalized silicon nanoparticles (3NM-Acid, 6NM-Acid and 9NM-Acid) were prepared as follows. SiNPs were added to the TMOS solution noted above with sonication for 1 min; then the precursor solutions were mixed together and sonicated for an additional 1 min, poured into molds and treated as described above. The same protocol was followed using polymer coated SiNPs (3NM-P, 9NM-P and 100NM-P).

5.1 Characterization of Aerogels

The aerogels were characterized by means of PL, TEM and nitrogen (N_2) adsorption/desorption isotherms. BET (Brunauer–Emmett–Teller) model was used to explain the adsorption/desorption isotherms.

6 RESULTS AND DISCUSSION: SILICA- AND NANOPARTICLE-DOPED AEROGELS

Silica aerogels were prepared by sol-gel processing. The process can be divided into three steps (Dorcheh and Abbasi 2008):

1. *Gel preparation*. The sol is prepared by a silica source solution and by addition of catalyst, gelation occurs. The gels are usually classified according to the dispersion medium used, e.g., hydrogel or aquagel, alcogel and aerogel (for water, alcohol, and air, respectively).
2. *Aging of the gel*. The gel prepared in the first step is aged in its mother solution. This aging process strengthens the gel, so that shrinkage during the drying step is kept to a minimum.
3. *Drying of the gel*. In this step, the gel is freed of the liquid in its pores to prevent the collapse of the gel structure.

One major challenge in the preparation of aerogels is to eliminate the solvent from gel without collapsing the already existing nanoporous structure and thereby avoiding the subsequent shrinkage and cracking of the dried gel. For the purposes of this study, aerogels were obtained upon drying using a home-built supercritical dryer shown in Figure 9. Xerogels were obtained *via* ambient condition solvent evaporation.

While silica aerogels are typically optically transparent, inclusion of SiNPs causes the resulting gels to appear opaque. It is possible some of this opacity arises because the nanoparticles are acting as scattering centers, however it may also result from localized surface reactions at the SiNP nuclei occurring during gel formation. Blank silica aerogels showed a weak blue photoluminescence upon exposure to UV light, while aerogels containing SiNPs showed characteristic photoluminescence of the nanoparticle component (i.e., orange, red, and no photoluminescence for 3NM-Acid, 6NM-Acid and 9NM-Acid SiNPs respectively; Figure 10). The nanoparticles remain immobilized within the gel structure and do not leach after repeated washings with various solvents, or during the supercritical drying.

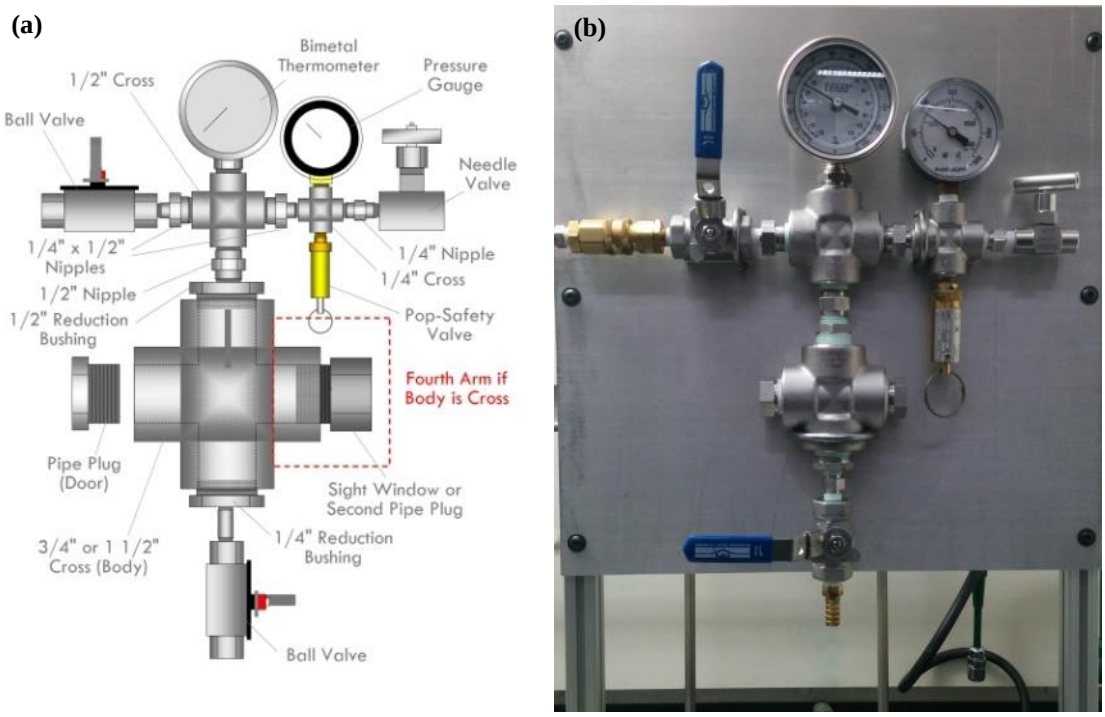

Figure 9. Supercritical dryer (a) Schematic and (b) the assembled version.

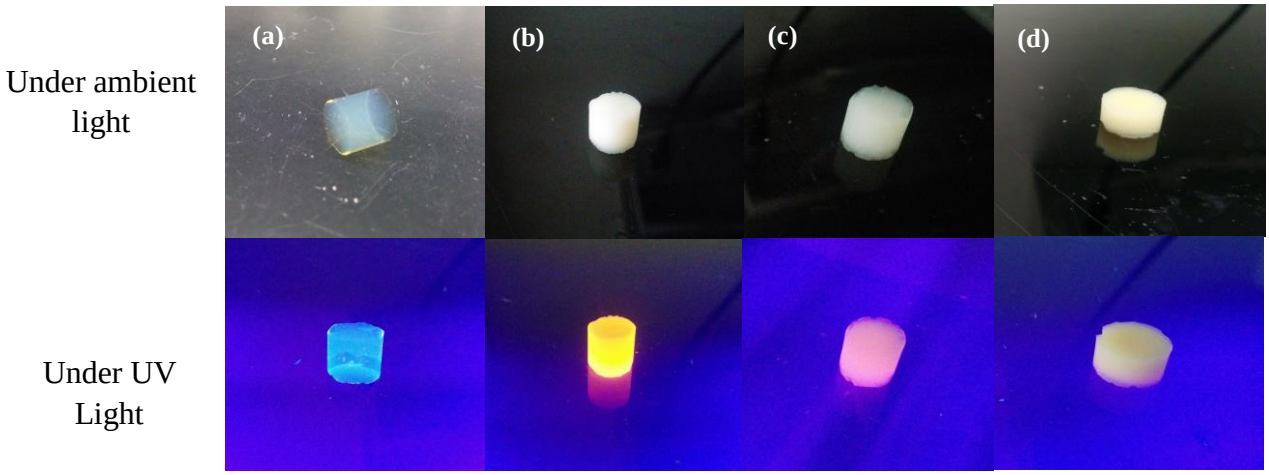

Figure 10. Silica aerogels.
(a) blank silica aerogel
(b) 3NM-Acid (c) 6NM-Acid and (d) 9NM-Acid hybrid aerogels containing pentanoic acid functionalized SiNPs under ambient and UV light.

The xerogel samples of silica showed visible cracking and shrinkage upon drying under ambient conditions indicating a loss of porosity (Figure 11).

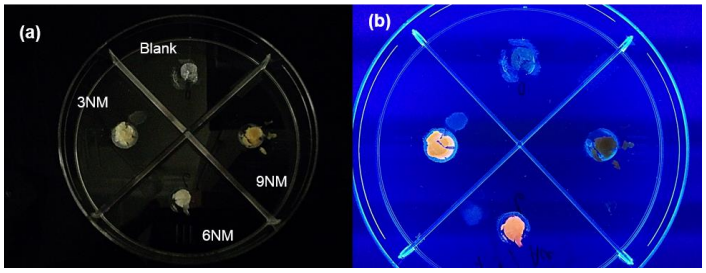

Figure 11. Silica based xerogels (blank and SiNPs containing hybrids). (a) ambient light; (b) UV light.

The aerogels were further characterized using TEM, however challenges related to sample preparation and nanoparticle imaging were encountered. Still, TEM images of the aerogel samples revealed empty mesopores with no long-range order (Figure 12). The blank silica aerogels showed continuous amorphous networks with mesoporous structure (Figure 12(a)). In contrast, xerogels samples show a collapse of porous network structure and no mesopores were detected (Figure 12(b)). Immobilization of SiNPs into the aerogels does not appear to disturb the internal structure of the aerogels (Figure 12(c to e)). Clearly, the SiNP/aerogel hybrids combine the low density and high surface area of aerogels with the optical characteristics of SiNPs.

Similarly, polymer intercalated 3NM-P, 9NM-P and 100NM-P were immobilized into the silica aerogels. The 3NM-P immobilized silica aerogels displayed characteristic colour under UV while 9NM-P and 100NM-P immobilized aerogels did not display any photoluminescence. The aerogels were stable and did not show any cracks (Figure 13).

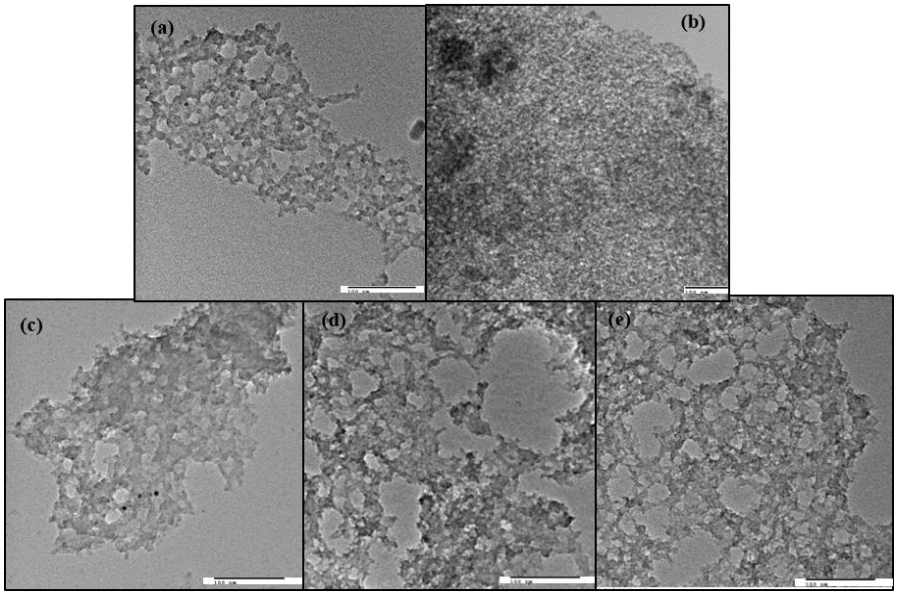

Figure 12. TEM images of silica aerogels.
(a) Blank aerogel (b) xerogel (c) 3NM-Acid (d) 6NM-Acid and (d) 9NM-Acid SiNPs immobilized aerogels.
Scale bar = 100 nm.

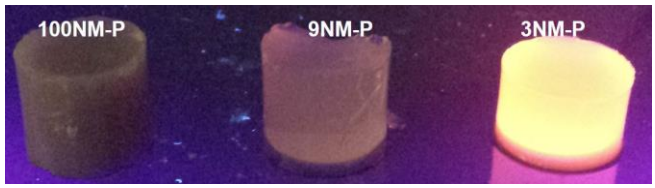

Figure 13. Silica aerogels impregnated with polymer intercalated SiNPs under UV light.

The micro and mesoporosity were confirmed by nitrogen physisorption measurements. The adsorption desorption isotherms show a type IV profile for blank xerogels with H1-type hysteresis loops characteristic of ink-bottle shaped pores with broad pore-size distribution. The blank aerogels and hybrid aerogels showed a type V isotherm with H3-type hysteresis loops characteristic of an interconnected mesoporous system having mesopores with cylindrical geometries (Figure 14).

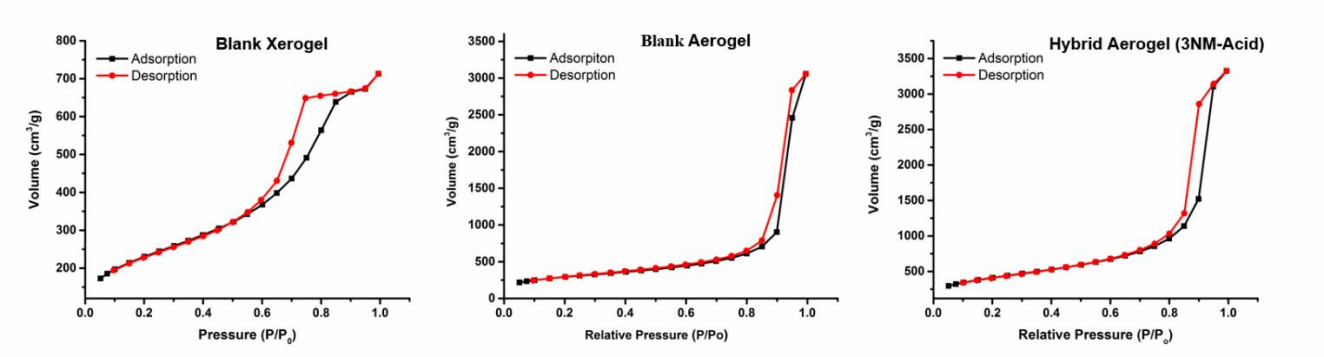

Figure 14. Nitrogen adsorption/desorption isotherms for xerogels, aerogel and hybrid aerogel samples respectively.

The adsorption/desorption isotherms also provided valuable information about the surface area, pore size and pore volume of the aerogels (Table 2). As expected, blank aerogels showed higher surface areas with a narrow pore sizes as compared to the blank xerogels. The hybrid aerogels showed highest surface area with narrow pore sizes.

Table 2. Structural properties of xerogels/aerogels obtained from the adsorption/desorption isotherms.

Sample	**Surface Area (m^2/g)**	**Pore Volume (cm^3/g)**	**Pore Size (nm)**
Xerogel (blank)	804.6	1.1	54.9
Aerogel (blank)	1,019	4.74	18.6
Aerogel (hybrid)	1,478	5.16	13.95

7 CONCLUSIONS AND RECOMMENDATIONS

7.1 Conclusions

SiNPs of different sizes were synthesized in high yields. The nanoparticles were rendered water-soluble by either intercalating with an amphiphilic polymer or by terminating them with carboxylic acids.

Silica aerogels were successfully synthesized *via* sol-gel processing and dried using an in-house supercritical dryer. The dried aerogels maintain their morphology without shrinking. Upon immobilization of SiNPs of different sizes, the aerogels do not lose their characteristic network structure and porosity. The aggregation of nanoparticles observed in TEM is most probably a

manifestation of sample preparation. The aerogels are composed of continuous networks of mesopores with very high surface area and porosity as confirmed by the adsorption/desorption isotherms.

The immobilization of photocatalytic SiNPs in/onto aerogel membranes is expected to offer several advantages compared to other approaches, including:

1. comparatively low energy and chemical usage,
2. production of water of consistent quality independent of the quality of the treated water,
3. automatic control and steady operation allowing continuous operation,
4. low maintenance costs, and
5. straightforward scalability through addition of membrane modules.

The use of SiNPs could assist in overcoming several disadvantages of TiO_2-based photocatalysts; for example, TiO_2 can only absorb 5% of solar spectrum energy due to its wide band gap and faster recombination rates making it an inefficient solar-based photocatalyst. The band gap of large Si nanoparticles allows absorption of more than 50% of the solar spectrum (Shockley and Queisser 1961) making passive solar-induced remediation of organic pollutants a viable option.

Silica and hybrid aerogels were designed with a well-developed and controlled micro- and mesoporosity, a narrow mesopore size distribution and a large surface area. These unique properties make them promising materials for applications in photocatalysis.

7.2 Recommendations

The following recommendations are put forth based on the current results and understanding of hybrid aerogels and photocatalytic activity of SiNPs:

1. Complete characterization of the aerogels is necessary. In particular, the microstructure of aerogels needs to be probed using advanced sampling techniques such as cryo-microtoming or focused ion beam milling (FIB). Such techniques will help resolve the actual distribution and structure of nanoparticles in the aerogels. This is essential for optimizing the structure-property relationship of the hybrid aerogels.
2. It is also recommended that SiNPs be immobilized onto the surfaces of the aerogels as compared to immobilization into the aerogels by developing proper functional groups and tailoring the sol-gel chemistry. Such tuning will help to increase the photocatalytic properties of the hybrid aerogels.
3. It is important that the photocatalytic activity of the hybrids be investigated for model compounds and that the scope of the studies be expanded to more complex molecules such as cyclohexanoic acid (CHA) or acids with multiple aromatic rings that serve as more accurate analogues of the naphthenic acids present in OSPW.

4. It is also recommended that aerogel hybrids be deployed in laboratory-scale reactors so that photocatalytic activity of the hybrid aerogels can be tested. The design and fabrication of laboratory-scale reactors will allow for effective evaluation of the efficacy of nanoparticles in OSPW degradation.

8 REFERENCES

Anderson, M.L., C.A. Morris, R.M. Stroud, C.I. Merzbacher and D.R. Rolison, 1999. Colloidal gold aerogels: Preparation, properties, and characterization. Langmuir 15(3): 674-681.

Celzard, A., V. Fierro and G. Amaral-Labat, 2012. Adsorption by carbon gels. Elsevier Ltd.

Chin, S.S., K. Chiang and A. G. Fane, 2006. The stability of polymeric membranes in a TiO_2 photocatalysis process. Journal of Membrane Science 275(1-2): 202-211.

Chong, M.N., B. Jin, C.W.K. Chow and C. Saint, 2010. Recent developments in photocatalytic water treatment technology: A review. Water Research 44(10): 2997-3027.

Chong, M.N., S. Lei, B. Jin, C. Saint and C.W.K. Chow, 2009. Optimisation of an annular photoreactor process for degradation of Congo Red using a newly synthesized titania impregnated kaolinite nano-photocatalyst. Separation and Purification Technology 67(3): 355-363.

Dorcheh, S.A. and M.H. Abbasi, 2008. Silica aerogel; synthesis, properties and characterization. Journal of Materials Processing Technology 199(1-3): 10-26.

García-González, C.A., M.C. Camino-Rey, M. Alnaief, C. Zetzl and I. Smirnova, 2012. Supercritical drying of aerogels using CO_2: Effect of extraction time on the end material textural properties. The Journal of Supercritical Fluids 66(0): 297-306.

Gesser, H.D. and P.C. Goswami, 1989. Aerogels and related porous materials. Chemical Reviews 89(4): 765-788.

Gogate, P.R. and A.B. Pandit, 2004. A review of imperative technologies for wastewater treatment I: oxidation technologies at ambient conditions. Advances in Environmental Research 8(3-4): 501-551.

Henderson, E.J., J.A. Kelly and J.G.C. Veinot, 2009. Influence of $HSiO_{1.5}$ sol-gel polymer structure and composition on the size and luminescent properties of silicon nanocrystals. Chemistry of Materials 21(22): 5426-5434.

Hessel, C.M., E.J. Henderson and J.G.C. Veinot, 2006. Hydrogen silsesquioxane: A molecular precursor for nanocrystalline $Si-SiO_2$ composites and freestanding hydride-surface-terminated silicon nanoparticles. Chemistry of Materials 18(26): 6139-6146.

Hessel, C.M., E.J. Henderson and J.G.C. Veinot, 2007. An investigation of the formation and growth of oxide-embedded silicon nanocrystals in hydrogen silsesquioxane-derived nanocomposites. Journal of Physical Chemistry C 111(19): 6956-6961.

Iqbal, M., T.K. Purkait, J.G.C. Veinot and G.G. Goss, 2013. Benign-by-design: Synthesis of engineered silicon nanoparticles and their application to oil sands water contaminant remediation. Oil Sands Research and Information Network, University of Alberta, School of

Energy and the Environment, Edmonton, Alberta. OSRIN Report No. TR-42. 30 pp. http://hdl.handle.net/10402/era.37308 [Last accessed October 28, 2014].

Jin, Y., M. Wu, G. Zhao and M. Li, 2011. Photocatalysis-enhanced electrosorption process for degradation of high-concentration dye wastewater on TiO_2/carbon aerogel. Chemical Engineering Journal 168(3): 1248-1255.

Kang, Z., C.H.A. Tsang, N-B. Wong, Z. Zhang and S-T. Lee, 2007. Silicon quantum dots: A general photocatalyst for reduction, decomposition, and selective oxidation reactions. Journal of the American Chemical Society 129(40): 12090-12091.

Kwak, S-Y., S.H. Kim and S.S. Kim, 2001. Hybrid organic/inorganic reverse osmosis (RO) membrane for bactericidal anti-fouling. 1. Preparation and characterization of TiO_2 nanoparticle self-assembled aromatic polyamide thin-film-composite (TFC) membrane. Environmental Science & Technology 35(11): 2388-2394.

Lee, D.K., S.C. Kim, I.C. Cho, S.J. Kim and S.W. Kim, 2004. Photocatalytic oxidation of microcystin-LR in a fluidized bed reactor having TiO_2-coated activated carbon. Separation and Purification Technology 34(1-3): 59-66.

Li, D., L. Wang and G. Zhang, 2013. A photocatalytic reactor derived from microstructured polymer optical fiber preform. Optics Communications 286(1): 182-186.

Lin, C.A.J., R.A. Sperling, J.K. Li, T.Y. Yang, P.Y. Li, M. Zanella, W.H. Chang and W.J. Parak, 2008. Design of an amphiphilic polymer for nanoparticle coating and functionalization. Small 4(3): 334-341.

Meena, A. K., G. K. Mishra, P. K. Rai, C. Rajagopal and P. N. Nagar, 2005. Removal of heavy metal ions from aqueous solutions using carbon aerogel as an adsorbent. Journal of Hazardous Materials 122(1-2): 161-170.

Mozia, S., 2010. Photocatalytic membrane reactors (PMRs) in water and wastewater treatment. A review. Separation and Purification Technology 73(2): 71-91.

Perdigoto, M.L.N., R.C. Martins, N. Rocha, M.J. Quina, L. Gando-Ferreira, R. Patrício and L. Durães, 2012. Application of hydrophobic silica based aerogels and xerogels for removal of toxic organic compounds from aqueous solutions. Journal of Colloid and Interface Science 380(1): 134-140.

Pozzo, R.L., M.A. Baltanás and A.E. Cassano, 1997. Supported titanium oxide as photocatalyst in water decontamination: State of the art. Catalysis Today 39(3): 219-231.

Qu, X., P.J.J. Alvarez and Q. Li, 2013. Applications of nanotechnology in water and wastewater treatment. Water Research 47(12): 3931-3946.

Qu, X., J. Brame, Q. Li and P.J.J. Alvarez, 2012. Nanotechnology for a safe and sustainable water supply: enabling integrated water treatment and reuse. Accounts of Chemical Research 46(3): 834-843.

Qu, Y. and X. Duan, 2013. Progress, challenge and perspective of heterogeneous photocatalysts. Chemical Society Reviews 42(7): 2568-2580.

Sánchez-Polo, M., J. Rivera-Utrilla, E. Salhi and U. von Gunten, 2006. Removal of bromide and iodide anions from drinking water by silver-activated carbon aerogels. Journal of Colloid and Interface Science 300(1): 437-441.

Shockley, W. and H. J. Queisser, 1961. Detailed balance limit of efficiency of p-n junction solar cells. Journal of Applied Physics 32(3): 510-519.

Sun, L. and J.R. Bolton, 1996. Determination of the quantum yield for the photochemical generation of hydroxyl radicals in TiO_2 suspensions. The Journal of Physical Chemistry 100(10): 4127-4134.

Veinot, J.G.C., 2006. Synthesis, surface functionalization, and properties of freestanding silicon nanocrystals. Chemical Communications (40): 4160-4168.

Wang, Z., L. Wang, L. Yao, M. Pei and G. Zhang, 2013. Membrane separation coupled with photocatalysis for water supply and wastewater treatment. Advanced Materials Research 671-674: 2571-2574.

Xi, W. and S.U. Geissen, 2001. Separation of titanium dioxide from photocatalytically treated water by cross-flow microfiltration. Water Research 35(5): 1256-1262.

Yang, G.C.C. and C-J. Li, 2007. Electrofiltration of silica nanoparticle-containing wastewater using tubular ceramic membranes. Separation and Purification Technology 58(1): 159-165.

Zaky, A.M. and B.P. Chaplin, 2013. Porous substoichiometric TiO_2 anodes as reactive electrochemical membranes for water treatment. Environmental Science & Technology 47(12): 6554-6563.

Zhai, Y., M. Dasog, R.B. Snitynsky, T.K. Purkait, M. Aghajamali, A.H. Hahn, C.B. Sturdy, T.L. Lowary and J. Veinot, 2014. Water-soluble photoluminescent D-mannose and L-alanine functionalized silicon nanocrystals and their application to cancer cell imaging. Journal of Materials Chemistry B (DOI: 10.1039/C4TB01161A).

Zhang, X., A.J. Du, P. Lee, D.D. Sun and J.O. Leckie, 2008. TiO_2 nanowire membrane for concurrent filtration and photocatalytic oxidation of humic acid in water. Journal of Membrane Science 313(1-2): 44-51.

Zhang, X., J.H. Pan, A.J. Du, W. Fu, D.D. Sun and J.O. Leckie, 2009. Combination of one-dimensional TiO_2 nanowire photocatalytic oxidation with microfiltration for water treatment. Water Research 43(5): 1179-1186.

Zhang, Y., X. Han, R. Liu, Y. Liu, H. Huang, J. Zhang, H. Yu and Z. Kang, 2012. Tunable Metal/Silicon Hybrid Dots Catalysts for Hydrocarbon Selective Oxidation. Journal of Physical Chemistry C 116(38): 20363-20367.

Zhu, H., X. Gao, Y. Lan, D. Song, Y. Xi and J. Zhao, 2004. Hydrogen titanate nanofibers covered with anatase nanocrystals: A delicate structure achieved by the wet chemistry reaction of the titanate nanofibers. Journal of the American Chemical Society 126(27): 8380-8381.

9 GLOSSARY

9.1 Definitions

Aerogel

Coherent, porous solids made by the formation of a colloidal gel followed by removal of the liquid from within the pores of the gel.

Amphiphile/Amphiphilic

A chemical compound possessing both hydrophilic (water-loving, polar) and hydrophobic (non-polar) characteristics.

Band Gap

The band gap of a semiconductor is the minimum energy required to excite an electron that is stuck in its bound state into a free state where it can participate in conduction.

Conduction Band

The energy level at which an electron can be considered free.

Hybrid Aerogel

Aerogels containing filler materials, such as nanoparticles, which show synergistic effects of their constituents.

Hydrosilylation

The addition of Si-H (silicon – hydrogen) bonds across unsaturated bonds (e.g., alkenes, alkynes, etc.).

Intercalation

Reversible inclusion of a molecule (or group) between two other molecules (or groups).

Microtoming (or cryo-microtoming)

Microtoming is an experimental technique for slicing ultrathin sections of a sample for microscopic examination.

The sectioning of frozen samples is carried out under liquid nitrogen and is termed as cryo-microtoming.

Moiety

A part or functional group of a molecule.

Monolith

A single large piece of a substance.

Nanocomposite

A two phase material that contains nanomaterials as fillers or reinforcement.

Nanocrystal

A solid particle that is a single crystal in the nanometre size range.

Nanoparticle

A solid particle or a material that has at least one dimension in the range of 1 to 100 nm.

Photocatalysis

A reaction which uses light to activate a substance which modifies the rate of a chemical reaction without being involved itself.

Photocatalyst

A chemical compound or substance that can modify the rate of a chemical reaction using light irradiation.

Photoexcitation

The process of electron excitation by light (photon) absorption.

Photoinduced

Any process caused by absorption of light.

Photoluminescence

Light emission from any form of matter after the absorption of light (photon).

Physisorption

The physical bonding of gas molecules to the surface of a solid or liquid that the gas comes into contact with at low temperatures. The weak, long-range bonding is not surface-specific and takes place between all gas molecules on any surface.

Scavenger

A substance added to a mixture to remove or inactivate impurities.

Sol-Gel

Process through which a network is formed from solution by a progressive change of liquid precursor(s) into a sol, to a gel, and in most cases finally to a dry network.

Stretching

Stretching of chemical bonds upon absorption of infrared (IR) radiations.

Tunability

The ability to tune or control properties of a material.

Valence Band (VB) Electron

The electrons present in the valence band (ground state).

Valence Band Hole

The hole (an empty state) created in the valence band after the electron jumps from valence band to the conduction band.

Xerogel

If the liquid within the gel is removed by simple evaporation, the resulting gel is termed a xerogel.

9.2 Acronyms

AOP	Advanced Oxidation Processes
BET	Brunauer–Emmett–Teller model (the name of three scientists who proposed the model)
ca.	circa (about)
CB	Conduction Band
nm	Nanometre
NPs	Nanoparticles
eV	Electron Volt
FIB	Focused Ion Beam
FTIR	Fourier-Transform Infrared Spectroscopy
HR-TEM	High Resolution Transmission Electron Microscopy
IR	Infrared
LC-MS	Liquid Chromatography – Mass Spectrometry
MS	Mass Spectrometry
NC	Nanocrystal
NPs	Nanoparticles
OSPW	Oil Sands Process-Affected Water
OSRIN	Oil Sands Research and Information Network
PL	Photoluminescence
PMR	Photocatalytic Membrane Reactor
PM(s)	Photocatalytic Membrane(s)
QY/QYs	Quantum Yield/s
ROS	Reactive Oxygen Species
SEE	School of Energy and the Environment

TEM	Transmission Electron Microscopy
UV	Ultraviolet
VB	Valence Band

9.3 Chemicals/Chemistry

Ar	Argon
Br^-	Bromide
C	Carbon
Cd	Cadmium
CHA	Cyclohexanoic Acid
CO_2	Carbon dioxide
Cu	Copper
H	Hydrogen
HF	Hydrofluoric Acid
HSQ	Hydrogen Silsesquioxane
I^-	Iodide
MeOH	Methanol
mg/L	Milligrams per litre
mM	Millimolar
Mn	Manganese
N	Nitrogen
NA / NAs	Naphthenic Acid / Naphthenic Acids
Ni	Nickle
O	Oxygen
$^{\bullet}OH$	Hydroxyl radical
PAH	Polycyclic Aromatic Hydrocarbon
Si	Silicon
SiNP(s)	Silicon nanoparticle(s)
SiO_2	Silica
TiO_2	Titanium dioxide
TMOS	Tetramethoxysilane

μL	Micro Litre
Zn	Zinc

LIST OF OSRIN REPORTS

OSRIN reports are available on the University of Alberta's Education & Research Archive at http://hdl.handle.net/10402/era.17209. The Technical Report (TR) series documents results of OSRIN funded projects. The Staff Reports (Bolton and Stefan) series represent work done by OSRIN staff.

OSRIN Technical Reports – http://hdl.handle.net/10402/era.17507

BGC Engineering Inc., 2010. Oil Sands Tailings Technology Review. OSRIN Report No. TR-1. 136 pp. http://hdl.handle.net/10402/era.17555

BGC Engineering Inc., 2010. Review of Reclamation Options for Oil Sands Tailings Substrates. OSRIN Report No. TR-2. 59 pp. http://hdl.handle.net/10402/era.17547

Chapman, K.J. and S.B. Das, 2010. Survey of Albertans' Value Drivers Regarding Oil Sands Development and Reclamation. OSRIN Report TR-3. 13 pp. http://hdl.handle.net/10402/era.17584

Jones, R.K. and D. Forrest, 2010. Oil Sands Mining Reclamation Challenge Dialogue – Report and Appendices. OSRIN Report No. TR-4. 258 pp. http://hdl.handle.net/10402/era.19092

Jones, R.K. and D. Forrest, 2010. Oil Sands Mining Reclamation Challenge Dialogue – Report. OSRIN Report No. TR-4A. 18 pp. http://hdl.handle.net/10402/era.19091

James, D.R. and T. Vold, 2010. Establishing a World Class Public Information and Reporting System for Ecosystems in the Oil Sands Region – Report and Appendices. OSRIN Report No. TR-5. 189 pp. http://hdl.handle.net/10402/era.19093

James, D.R. and T. Vold, 2010. Establishing a World Class Public Information and Reporting System for Ecosystems in the Oil Sands Region – Report. OSRIN Report No. TR-5A. 31 pp. http://hdl.handle.net/10402/era.19094

Lott, E.O. and R.K. Jones, 2010. Review of Four Major Environmental Effects Monitoring Programs in the Oil Sands Region. OSRIN Report No. TR-6. 114 pp. http://hdl.handle.net/10402/65.20287

Godwalt, C., P. Kotecha and C. Aumann, 2010. Oil Sands Tailings Management Project. OSRIN Report No. TR-7. 64 pp. http://hdl.handle.net/10402/era.22536

Welham, C., 2010. Oil Sands Terrestrial Habitat and Risk Modeling for Disturbance and Reclamation – Phase I Report. OSRIN Report No. TR-8. 109 pp. http://hdl.handle.net/10402/era.22567

Schneider, T., 2011. Accounting for Environmental Liabilities under International Financial Reporting Standards. OSRIN Report TR-9. 16 pp. http://hdl.handle.net/10402/era.22741

Davies, J. and B. Eaton, 2011. Community Level Physiological Profiling for Monitoring Oil Sands Impacts. OSRIN Report No. TR-10. 44 pp. http://hdl.handle.net/10402/era.22781

Hurndall, B.J., N.R. Morgenstern, A. Kupper and J. Sobkowicz, 2011. Report and Recommendations of the Task Force on Tree and Shrub Planting on Active Oil Sands Tailings Dams. OSRIN Report No. TR-11. 15 pp. http://hdl.handle.net/10402/era.22782

Gibson, J.J., S.J. Birks, M. Moncur, Y. Yi, K. Tattrie, S. Jasechko, K. Richardson, and P. Eby, 2011. Isotopic and Geochemical Tracers for Fingerprinting Process-Affected Waters in the Oil Sands Industry: A Pilot Study. OSRIN Report No. TR-12. 109 pp. http://hdl.handle.net/10402/era.23000

Oil Sands Research and Information Network, 2011. Equivalent Land Capability Workshop Summary Notes. OSRIN Report TR-13. 83 pp. http://hdl.handle.net/10402/era.23385

Kindzierski, W., J. Jin and M. Gamal El-Din, 2011. Plain Language Explanation of Human Health Risk Assessment. OSRIN Report TR-14. 37 pp. http://hdl.handle.net/10402/era.23487

Welham, C. and B. Seely, 2011. Oil Sands Terrestrial Habitat and Risk Modelling for Disturbance and Reclamation – Phase II Report. OSRIN Report No. TR-15. 93 pp. http://hdl.handle.net/10402/era.24547

Morton Sr., M., A. Mullick, J. Nelson and W. Thornton, 2011. Factors to Consider in Estimating Oil Sands Plant Decommissioning Costs. OSRIN Report No. TR-16. 62 pp. http://hdl.handle.net/10402/era.24630

Paskey, J. and G. Steward, 2012. The Alberta Oil Sands, Journalists, and Their Sources. OSRIN Report No. TR-17. 33 pp. http://hdl.handle.net/10402/era.25266

Cruz-Martinez, L. and J.E.G. Smits, 2012. Potential to Use Animals as Monitors of Ecosystem Health in the Oil Sands Region – July 2013 Update. OSRIN Report No. TR-18. 59 pp. http://hdl.handle.net/10402/era.25417

Hashisho, Z., C.C. Small and G. Morshed, 2012. Review of Technologies for the Characterization and Monitoring of VOCs, Reduced Sulphur Compounds and CH_4. OSRIN Report No. TR-19. 93 pp. http://hdl.handle.net/10402/era.25522

Kindzierski, W., J. Jin and M. Gamal El-Din, 2012. Review of Health Effects of Naphthenic Acids: Data Gaps and Implications for Understanding Human Health Risk. OSRIN Report No. TR-20. 43 pp. http://hdl.handle.net/10402/era.26060

Zhao, B., R. Currie and H. Mian, 2012. Catalogue of Analytical Methods for Naphthenic Acids Related to Oil Sands Operations. OSRIN Report No. TR-21. 65 pp. http://hdl.handle.net/10402/era.26792

Oil Sands Research and Information Network and Canadian Environmental Assessment Agency, 2012. Summary of the Oil Sands Groundwater – Surface Water Interactions Workshop. OSRIN Report No. TR-22. 125 pp. http://hdl.handle.net/10402/era.26831

Valera, E. and C.B. Powter, 2012. Implications of Changing Environmental Requirements on Oil Sands Royalties. OSRIN Report No. TR-23. 21 pp. http://hdl.handle.net/10402/era.27344

Dixon, R., M. Maier, A. Sandilya and T. Schneider, 2012. Qualifying Environmental Trusts as Financial Security for Oil Sands Reclamation Liabilities. OSRIN Report No. TR-24. 32 pp. http://hdl.handle.net/10402/era.28305

Creasey, R., 2012. Professional Judgment in Mineable Oil Sands Reclamation Certification: Workshop Summary. OSRIN Report No. TR-25. 52 pp. http://hdl.handle.net/10402/era.28331

Alberta Innovates – Technology Futures, 2012. Investigating a Knowledge Exchange Network for the Reclamation Community. OSRIN Report No. TR-26. 42 pp. http://hdl.handle.net/10402/era.28407

Dixon, R.J., J. Kenney and A.C. Sandilya, 2012. Audit Protocol for the Mine Financial Security Program. OSRIN Report No. TR-27. 27 pp. http://hdl.handle.net/10402/era.28514

Davies, J., B. Eaton and D. Humphries, 2012. Microcosm Evaluation of Community Level Physiological Profiling in Oil Sands Process Affected Water. OSRIN Report No. TR-28. 33 pp. http://hdl.handle.net/10402/era.29322

Thibault, B., 2012. Assessing Corporate Certification as Impetus for Accurate Reporting in Self-Reported Financial Estimates Underlying Alberta's Mine Financial Security Program. OSRIN Report No. TR-29. 37 pp. http://hdl.handle.net/10402/era.29361

Pyper, M.P., C.B. Powter and T. Vinge, 2013. Summary of Resiliency of Reclaimed Boreal Forest Landscapes Seminar. OSRIN Report No. TR-30. 131 pp. http://hdl.handle.net/10402/era.30360

Pyper, M. and T. Vinge, 2013. A Visual Guide to Handling Woody Materials for Forested Land Reclamation. OSRIN Report No. TR-31. 10 pp. http://hdl.handle.net/10402/era.30381

Mian, H., N. Fassina, A. Mukherjee, A. Fair and C.B. Powter, 2013. Summary of 2013 Tailings Technology Development and Commercialization Workshop. OSRIN Report No. TR-32. 69 pp. http://hdl.handle.net/10402/era.31012

Howlett, M. and J. Craft, 2013. Application of Federal Legislation to Alberta's Mineable Oil Sands. OSRIN Report No. TR-33. 94 pp. http://hdl.handle.net/10402/era.31627

Welham, C., 2013. Factors Affecting Ecological Resilience of Reclaimed Oil Sands Uplands. OSRIN Report No. TR-34. 44 pp. http://hdl.handle.net/10402/era.31714

Naeth, M.A., S.R. Wilkinson, D.D. Mackenzie, H.A. Archibald and C.B. Powter, 2013. Potential of LFH Mineral Soil Mixes for Land Reclamation in Alberta. OSRIN Report No. TR-35. 64 pp. http://hdl.handle.net/10402/era.31855

Welham, C. and B. Seely, 2013. Oil Sands Terrestrial Habitat and Risk Modelling for Disturbance and Reclamation: The Impact of Climate Change on Tree Regeneration and Productivity – Phase III Report. OSRIN Report No. TR-36. 65 pp. http://hdl.handle.net/10402/era.31900

Eaton, B., T. Muhly, J. Fisher and S-L. Chai, 2013. Potential Impacts of Beaver on Oil Sands Reclamation Success – an Analysis of Available Literature. OSRIN Report No. TR-37. 65 pp. http://hdl.handle.net/10402/era.32764

Paskey, J., G. Steward and A. Williams, 2013. The Alberta Oil Sands Then and Now: An Investigation of the Economic, Environmental and Social Discourses Across Four Decades. OSRIN Report No. TR-38. 108 pp. http://hdl.handle.net/10402/era.32845

Watson, B.M. and G. Putz, 2013. Preliminary Watershed Hydrology Model for Reclaimed Oil Sands Sites. OSRIN Report No. TR-39. 193 pp. http://hdl.handle.net/10402/era.34250

Birks, S.J., Y. Yi, S. Cho, J.J. Gibson and R. Hazewinkel, 2013. Characterizing the Organic Composition of Snow and Surface Water in the Athabasca Region. OSRIN Report No. TR-40. 62 pp. http://hdl.handle.net/10402/era.36643

De Corby, R.G., 2013. Development of Silicon-Based Optofluidic Sensors for Oil Sands Environmental Monitoring. OSRIN Report No. TR-41. 19 pp. http://hdl.handle.net/10402/era.36936

Iqbal, M., T.K. Purkait, J.G.C. Veinot and G.G. Goss, 2013. Benign-by-Design: Synthesis of Engineered Silicon Nanoparticles and their Application to Oil Sands Water Contaminant Remediation. OSRIN Report No. TR-42. 30 pp. http://hdl.handle.net/10402/era.37308

Oil Sands Research and Information Network, 2013. Future of Shrubs in Oil Sands Reclamation Workshop. OSRIN Report No. TR-43. 71 pp. http://hdl.handle.net/10402/era.37440

Smreciu, A., K. Gould and S. Wood, 2013. Boreal Plant Species for Reclamation of Athabasca Oil Sands Disturbances. OSRIN Report No. TR-44. 23 pp. plus appendices. http://hdl.handle.net/10402/era.37533

Pereira, A.S. and J.W. Martin, 2014. On-Line Solid Phase Extraction – HPLC – Orbitrap Mass Spectrometry for Screening and Quantifying Targeted and Non-Targeted Analytes in Oil Sands Process-Affected Water and Natural Waters in the Athabasca Oil Sands Region. OSRIN Report No. TR-45. 33 pp. http://hdl.handle.net/10402/era.37793

Liang, J., F. Tumpa, L.P. Estrada, M. Gamal El-Din and Y. Liu, 2014. Ozone-Assisted Settling of Diluted Oil Sands Mature Fine Tailings: A Mechanistic Study. OSRIN Report No. TR-46. 43 pp. http://hdl.handle.net/10402/era.38226

Rochdi, N., J. Zhang, K. Staenz, X. Yang, D. Rolfson, J. Banting, C. King and R. Doherty, 2014. Monitoring Procedures for Wellsite, In-Situ Oil Sands and Coal Mine Reclamation in Alberta. OSRIN Report No. TR-47. 156 pp. http://hdl.handle.net/10402/era.38742

Taheriazad, L., C. Portillo-Quintero and G.A. Sanchez-Azofeifa, 2014. Application of Wireless Sensor Networks (WSNs) to Oil Sands Environmental Monitoring. OSRIN Report No. TR-48. 51 pp. http://hdl.handle.net/10402/era.38858

Marey, H.S., Z. Hashisho and L. Fu, 2014. Satellite Remote Sensing of Air Quality in the Oil Sands Region. OSRIN Report No. TR-49. 104 pp. http://hdl.handle.net/10402/era.38882

Li, C., A. Singh, N. Klamerth, K. McPhedran, P. Chelme-Ayala, M. Belosevic and M. Gamal El-Din, 2014. Synthesis of Toxicological Behavior of Oil Sands Process-Affected Water Constituents. OSRIN Report No. TR-50. 101 pp. http://hdl.handle.net/10402/era.39659

Jiang, Y. and Y. Liu, 2014. Application of Forward Osmosis Membrane Technology for Oil Sands Process-Affected Water Desalination. OSRIN Report No. TR-51. 27 pp. http://hdl.handle.net/10402/era.39855

Zhu, L., M. Yu, L. Delgado Chávez, A. Ulrich and T. Yu, 2014. Review of Bioreactor Designs Applicable to Oil Sands Process-Affected Water Treatment. OSRIN Report No. TR-52. 39 pp. http://hdl.handle.net/10402/era.39903

Oil Sands Research and Information Network, 2014. Oil Sands Rules, Tools and Capacity: Are we Ready for Upcoming Challenges? OSRIN Report No. TR-53. 120 pp. http://hdl.handle.net/10402/era.39985

OSRIN Videos – http://hdl.handle.net/10402/era.29304

Rooney Productions, 2012. Assessment Methods for Oil Sands Reclamation Marshes. OSRIN Video No. V-1. 20 minutes. Also available on the University of Alberta You Tube Channel (recommended approach).

Rooney Productions, 2012. Assessment Methods for Oil Sands Reclamation Marshes. OSRIN Video No. V-1. Nine-part mobile device version. Also available on the University of Alberta You Tube Channel (link to Part 1 - recommended approach).

OSRIN Staff Reports – http://hdl.handle.net/10402/era.19095

OSRIN, 2010. Glossary of Terms and Acronyms used in Oil Sands Mining, Processing and Environmental Management – December 2013 Update. OSRIN Report No. SR-1. 123 pp. http://hdl.handle.net/10402/era.17544

OSRIN, 2010. OSRIN Writer's Style Guide – November 2013 Update. OSRIN Report No. SR-2. 29 pp. http://hdl.handle.net/10402/era.17545

OSRIN, 2010. OSRIN Annual Report: 2009/2010. OSRIN Report No. SR-3. 27 pp. http://hdl.handle.net/10402/era.17546

OSRIN, 2010. Guide to OSRIN Research Grants and Services Agreements - June 2011 Update. OSRIN Report No. SR-4. 21 pp. http://hdl.handle.net/10402/era.17558

OSRIN, 2011. Summary of OSRIN Projects – October 2014 Update. OSRIN Report No. SR-5. 113 pp. http://hdl.handle.net/10402/era.20529

OSRIN, 2011. OSRIN Annual Report: 2010/11. OSRIN Report No. SR-6. 34 pp. http://hdl.handle.net/10402/era.23032

OSRIN, 2011. OSRIN's Design and Implementation Strategy. OSRIN Report No. SR-7. 10 pp. http://hdl.handle.net/10402/era.23574

OSRIN, 2012. OSRIN Annual Report: 2011/12. OSRIN Report No. SR-8. 25 pp. http://hdl.handle.net/10402/era.26715

OSRIN, 2013. OSRIN Annual Report: 2012/13. OSRIN Report No. SR-9. 56 pp. http://hdl.handle.net/10402/era.31211

OSRIN, 2014. OSRIN Annual Report: 2013/14. OSRIN Report No. SR-10. 66 pp. http://hdl.handle.net/10402/era.38508